Eur. Phys. J. Spec. Top.
https://doi.org/10.1140/epjs/s11734-024-01107-4

THE EUROPEAN PHYSICAL JOURNAL SPECIAL TOPICS

Review

Soft and Living Matter: a perspective

Supurna Sinha[a]

Raman Research Institute, Bengaluru 560080, India

Received 26 September 2023 / Accepted 22 January 2024

Abstract This review article offers a perspective on Soft Matter, keeping Brownian motion, one of the foundational pillars of statistical mechanics and Soft Matter physics at the centerstage. The article unfolds with a class of pioneering experiments in the domain of Soft Matter. It focuses on a few topics on Soft Matter such as Brownian motion on curved surfaces, biopolymer elasticity, active Brownian motion to name a few. The concluding section ends with a perspective, connecting the apparently dissimilar topics of the review.

1 Introduction

Soft Matter is entropy-dominated matter. There are many everyday examples of Soft Matter: colloids like milk, ink and smoke, emulsions like mayonnaise, whipped cream, shampoo and shaving cream, viscoelastic materials like ketchup and toothpaste, to name a few. Foams, bubbles, polymers, micelles, monolayers, bilayers are examples of Soft Matter [1]. In recent years, an interface has emerged between Soft Matter and Living Matter. Examples of Living Matter are DNA and other biopolymers, fluid membranes which form the cell membranes and so on. Research in the area of Living Matter can be divided into two parts: in the first part, one investigates the physical properties of Living Matter—for instance, Biopolymer Elasticity and in the second part, a newer field, in which one studies the active aspect of Living Matter, like bacterial tumbling and running [2].

Soft Matter is a vast area of research. In this review article, we will restrict our canvas to a few topics in Soft and Living Matter. In the next section, we will briefly sketch a set of pioneering experiments in the field of Soft Matter [3] and then in subsequent sections will dwell on a few specific topics. One of the significant features of these experiments is that these stemmed from observing simple, everyday materials and the experimental setups were also relatively simple. Soft Matter, thus, provides a playing ground for unraveling deep physical concepts and ideas from simple, everyday observations. The unifying idea connecting the apparently dissimilar topics discussed here is Brownian motion [4], a fundamental pillar of statistical mechanics and Soft Matter. Brownian motion is the random motion of particles suspended in a fluid. This motion is named after the botanist Robert Brown, who noticed this phenomenon in 1827 while looking at pollen grains suspended in water through a microscope. Initially, it was conjectured that this random motion is a result of the Living Matter in pollen. It was eventually ruled out by carrying out the same experiment with inanimate matter. In 1905, Albert Einstein, in one of his major scientific contributions, put forward a theory of Brownian motion which is considered to be one of the landmark papers in the realm of Statistical Mechanics and Soft Matter. In Sect. 2, we highlight a set of pioneering experiments in the domain of Soft Matter physics. This section gives a perspective on the groundbreaking experimental contribution of Agnes Pockels to the realm of Soft Matter. Section 3 deals with Brownian motion on a sphere which has applications to a variety of Soft Matter systems. Sect. 4 deals with Biopolymer Elasticity, specifically the worm-like chain (WLC) model. The worm-like chain model is a model of an inextensible semiflexible polymer which maps to the problem of Brownian motion on a sphere. In particular, the tangent vectors to the curve representing the polymer form a unit sphere and the problem reduces to studying Brownian motion on the unit sphere, which can be handled by standard operator techniques familiar from quantum mechanics [5, 6]. Section 5 deals with active Brownian motion. Thus, the topics ranging over Brownian motion on a sphere, the WLC polymer model and active Brownian motion are woven together by the common theme of Brownian motion. Finally, we end the review with a few concluding remarks in Sect. 6.

[a] e-mail: supurna@rri.res.in (corresponding author)

Published online: 17 February 2024

2 Agnes Pockels's experiments: early examples of Soft Matter experiments

Agnes Pockels (14 February 1862–21 November 1935) was a German chemist who carried out experiments which played a crucial role in understanding properties of interfaces and are some of the earliest examples of Soft Matter experiments [3].

Pockels got interested in the effect of soap on water and the effect of impurities on water and soapy water while washing dishes as part of her domestic chores. Her experiments designed to understand the interplay of soap, water and impurities were carried out at home when she was about eighteen.

Pockels devised a metallic rectangular slide trough for making quantitative measurements on the surface properties of soapy water and related substances. The trough was filled with water. A metal strip was laid on top of the water across the width of the trough which divided the surface of the water in two parts. A ruler was placed along the length of the trough so that the position of the metal strip, and therefore the surface area of each of the two parts of the trough, could be determined as the strip was moved along the length of the trough.

Pockels also devised a direct measure of surface tension by placing a small disk on the surface of the water in the trough, and then by using a weighing scale to measure the weight necessary to lift the disk from the water. She compared the forces required to lift the disk from pure water to water containing impurities leading to a direct measure of surface tension. This apparatus led to an investigation of the surface forces of a variety of substances ranging between mono-molecular films, the surface tension of emulsions and solutions, and the effect of impurities on the physical properties of water. Pockels's design eventually led to the modern day Langmuir–Blodgett trough which is extensively used in colloid and surface science.

3 Brownian motion on a sphere

In this section, we will discuss Brownian motion on a sphere [7, 8]. Consider a particle diffusing on a sphere. If the diffusing particle returns to its starting point at time β its path subtends a solid angle Ω at the center of the sphere. We ask: what is the probability distribution of Ω ? More generally, consider a diffusing particle starting from the north pole of a sphere at time $\tau = 0$. Let us join the final position of the particle at time β to its initial one (the north pole) by the shorter geodesic. This rule is well defined, unless the final position is exactly at the south pole, a zero-probability event. The path followed by the diffusing particle (closed by the geodesic rule) encloses a solid angle Ω. The question we address is: At time β, what is the distribution $P_\beta(\Omega)$ of solid angles? An experimental motivation for this question comes from time-resolved fluorescence studies [9] on the Brownian motion of rod-like molecules on curved surfaces such as micelles and lipid vesicles. The experimentally measured fluorescence anisotropy is affected by the curvature of the surface due to geometric phase effects [10]. The problem of diffusion on curved surfaces reappears in nuclear magnetic resonance (NMR) and electron spin resonance (ESR) studies on micelles and lipid vesicles. The curvature of the surface affects the spin relaxation times [11]. In biological systems, the translational diffusion of solutes bound to various curved surfaces influences metabolic rates and transmission rates of chemical signals [9]. Fluorescence anisotropy decay of molecules on curved surfaces has been studied theoretically and using Monte Carlo simulations [9]. This study shows that the geometric phase crucially affects the anisotropy decay if the molecules are tilted relative to the surface normal. Thus one needs to theoretically determine the distribution of geometric phases or equivalently, the distribution of solid angles in order to understand diffusion processes on curved surfaces.

Before addressing this problem which comes up in many problems involving curved surfaces in Soft Matter physics, let us address a closely related problem [12]. which appears in the context of polymer entanglement, another Soft Matter problem. The question of interest is the following: given that a Brownian path on the plane is closed at time t, what is the probability that it encloses a given area A? Here, we discuss a general method of solving these problems using a connection between Brownian motion and magnetism [7]. The qualitative idea is to use a magnetic field as a 'counter', to measure the area enclosed in a Brownian motion. This leads to a relation between the distribution of areas in a Brownian motion and the partition function of a magnetic system, which can be used to cast light on both subjects. Here we will restrict our discussion only to Brownian motion which is of significance in the domain of Soft Matter, without touching upon magnetism which lies primarily in the realm of hard condensed matter. We first discuss the planar problem [13]. We then go on to discuss the problem of diffusion on the sphere.

Let a diffusing particle start from the origin $\mathbf{r} = 0$ of the plane at time $\tau = 0$. Let us suppose that the particle arrives at $\mathbf{r}_f$ at time β. Let us join $\mathbf{r}_f$ to the origin by a straight line. The open Brownian path $\mathbf{r}(\tau)$ closed by a straight line encloses an area A. What is the probability distribution $P(A)$ of areas? By 'area' we mean the algebraic area, including sign. Area enclosed to the left of the diffusing particle counts as positive and area to the right as negative.

Let $\{\mathbf{r}(\tau) = \{x(\tau), y(\tau)\}, 0 \leq \tau \leq \beta, \mathbf{r}(0) = \mathbf{0}\}$ be a realization of a Brownian path on the plane which starts at the origin. As is well known, Brownian paths are distributed according to the Wiener Measure [14]: if $F[\mathbf{r}(\tau)]$ is any functional on paths, the expectation value of F is given by

$$< F[\mathbf{r}(\tau)] >_W := \frac{\int \mathrm{d}\mathbf{r}_{\ f} \int D[\mathbf{r}(\boldsymbol{\emptyset})] F[\mathbf{r}(\tau)] \exp\left[-\int_0^\beta \{\frac{1}{2}\frac{\mathrm{d}\mathbf{r}}{\mathrm{d}\tau}.\frac{\mathrm{d}\mathbf{r}}{\mathrm{d}\tau}\mathrm{d}\tau\}\right]}{\int \mathrm{d}\mathbf{r}_{\ f} \int D[\mathbf{r}(\boldsymbol{\emptyset})] \exp\left[-\int_0^\beta \{\frac{1}{2}\frac{\mathrm{d}\mathbf{r}}{\mathrm{d}\tau}.\frac{\mathrm{d}\mathbf{r}}{\mathrm{d}\tau}\mathrm{d}\tau\}\right]} \tag{1}$$

In Eq. (1), the symbol $D[\mathbf{r}(\boldsymbol{\emptyset})]$ denotes a functional integral [5] over all paths which start at the origin and end at $\mathbf{r}_{\ f}$. Finally, the endpoint $\mathbf{r}_{\ f}$ is also integrated over. (We set the diffusion constant equal to half.) β is the time for which the diffusion has occurred [14]. Let $\mathcal{A}[\mathbf{r}(\tau)]$ be the algebraic area enclosed by the path $\mathbf{r}(\tau)$. Clearly, the normalized probability distribution of areas $P(A)$ is given by

$$P(A) :=< \delta(\mathcal{A}[\mathbf{r}(\tau)] - A) >_W . \tag{2}$$

It is convenient to consider the generating function $\tilde{P}(B)$ of the distribution $P(A)$:

$$\tilde{P}(B) := \overline{e^{iBA}} = \int P(A) e^{iBA} \mathrm{d}A, \tag{3}$$

which is the Fourier transform of $P(A)$ and one can recover $P(A)$ by taking an inverse Fourier transform of $\tilde{P}(B)$. Combining Eqs. (2) and (3) we get:

$$\tilde{P}(B) =< e^{iB\mathcal{A}} >_W . \tag{4}$$

By introducing a fictitious vector potential $\mathbf{A}$ pertaining to a flux $\oint \mathbf{A}.d\mathbf{r} = B\mathcal{A}$, we can recast Eq.(4) as follows [8]:

$$\tilde{P}(B) = \frac{Y(B)}{Y(0)}, \tag{5}$$

where $Y(B)$ is given by $Y(B) = \int d\mathbf{r}_f K^B(\mathbf{0}, \mathbf{r}_f)$ where $K^B(\mathbf{0}, \mathbf{r_f})$ is the quantum amplitude for a particle of unit charge and mass to go from $\mathbf{0}$ to $\mathbf{r}_f$ in imaginary time β in the presence of a homogeneous magnetic field. One can express $K^B(\mathbf{0}, \mathbf{r}_f)$ in terms of the eigenvalues and the eigenfunctions [8] and arrive at the following expression for $Y(B)$:

$$Y(B) = \frac{2\pi}{\cosh\left(\frac{\beta B}{2}\right)},$$

which leads to $\tilde{P}(B) = [\cosh(\frac{\beta B}{2})]^{-1}$. The Fourier transform of $\tilde{P}(B)$ gives us the distribution of areas:

$$P(A) = \left[\beta \cosh\left(\frac{\pi A}{\beta}\right)\right]^{-1}.$$

The above discussion of the distribution of areas for Brownian motion on a plane sets the stage for discussion of the central question addressed at the beginning of this section: what is the distribution $P(\Omega)$ of solid angles (Ω) enclosed by a Brownian particle starting at time $\tau = 0$ at the north pole $\hat{r}_n$ of a unit sphere and ending at any other point $\hat{r}_f$ on the sphere, the final point being joined to the initial one by a geodesic? (As stated earlier, this rule breaks down only if the final point is the south pole, which is a zero-probability event.) Unlike the planar case, $P(\Omega)$ is a periodic function with period 4π. The generating function $\tilde{P}_g$ of the distribution of solid angles is given by

$$\tilde{P}_g = \int_0^{4\pi} \mathrm{d}\Omega P(\Omega) e^{ig\Omega}$$

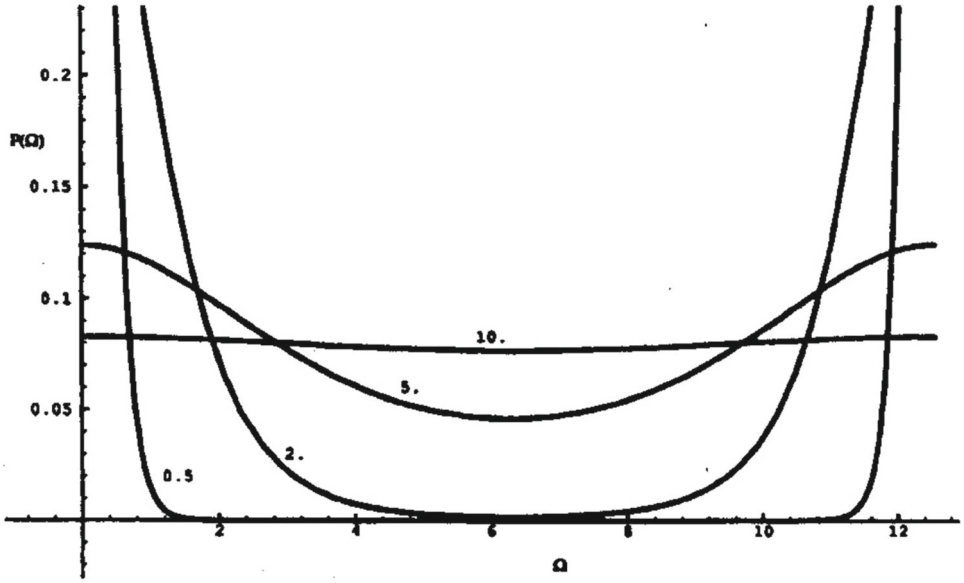

Fig. 1 Plots of $P(\Omega)$ versus Ω for various values of β indicated next to the plots

with g a half integer. In the Fourier domain, we have

$$P(\Omega) = \frac{1}{4\pi} \sum_{g=-\infty}^{\infty} e^{-ig\Omega} \tilde{P}_g.$$

Following steps similar to the case of the probability distribution of areas on a plane, we can express $\tilde{P}_g$ in terms of the eigenvalues and eigenfunctions of the corresponding magnetic problem, a quantum particle of unit charge on a sphere subject to a magnetic field created by a monopole of quantized strength g [7] at the center of the sphere.

Here we display the final expression for $P(\Omega)$:

$$P(\Omega) = \left(\frac{1}{4\pi}\right)\left(1 + 2\sum_{g=\frac{1}{2}}^{\infty} \cos(\Omega g)\tilde{P}_g\right), \tag{6}$$

where g increases in half-integer steps. The function displayed in Eq. (6) has been plotted for various values of β in Fig. 1. The plots show that for small values of the total time β the particle tends to make small excursions and its path encloses solid angles close to 0 or 4π and consequently the plots are peaked around these two values. As the available time β increases, other values of Ω are also probable and the peaks tend to spread and the curves flatten out. Finally in the limit of $\beta \to \infty$ the particle has enough time to enclose all possible solid angles with equal probability.

4 Biopolymer elasticity: the worm-like chain (WLC) model

4.1 Statistical mechanics of WLC

Polymers of different flexibilities are vital to life. Some polymers are as stiff as needles, others are as flexible as thread and still others are like twine, neither too stiff nor too floppy. The cytoskeletal structure of the cell, which gives rigidity to the cell, consists of semiflexible polymers like actin, microtubules, and intermediate filaments. The polymer which carries the genetic code, the DNA, is a semiflexible polymer. A typical human DNA in a cell is about a meter long and it is rather amazing that such a long molecule is packed into a cell nucleus of the size of a few microns. This efficient packaging is a mystery and raises questions about the elasticity of DNA [2]. DNA also assumes various different forms depending on the function it needs to perform—for instance, it is unwound during replication so that the genetic code can be accessed and copied [15]. At other times, the DNA assumes a supercoiled

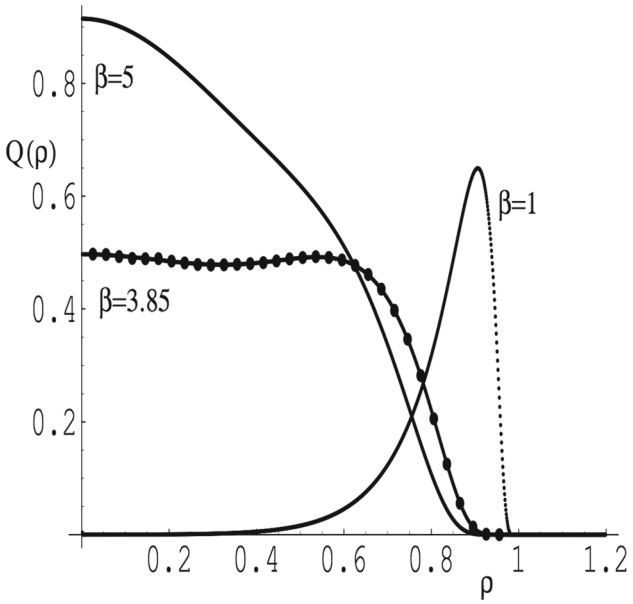

Fig. 2 Plots of the end-to-end distance vector distribution function $Q(\rho)$ of a WLC polymer versus the end-to-end distance vector ρ for various values of the ratio β of the contour length L to the persistence length L_P

configuration which protects and preserves the genetic code intact till it is needed. Such conformationally distinct configurations are also dictated by its elasticity.

Experimental studies of biopolymer molecules such as DNA have traditionally been limited to samples containing large numbers of molecules. This made it hard to probe the elastic properties of individual biopolymers which are of vital importance to biological processes such as protein-induced DNA bending [16]. It is only in the last couple of decades, due to advances in technology that single-molecule studies [17] became feasible. It is now possible to design experiments in which single molecules are pulled, stretched, and twisted to measure elastic properties [18]. In a typical single-molecule experiment, one considers a polymer molecule suspended between a fixed surface and a force sensor of some kind. The force sensor is a bead in a laser trap or a flexible cantilever of an atomic force microscope and the molecule under consideration can range from a DNA in a simple random coil configuration to a globular protein in a unique three-dimensionally folded form. For instance, one can study the "equation of state" of a semiflexible polymer by measuring its extension as a function of applied force. One can also tag the ends with fluorescent dye and determine the distribution of end-to-end distances (see Fig. 2) [6]. We learn a lot from such experimental studies about biologically relevant mechanical properties of these polymers. Such single-molecule micromanipulation studies have opened up a vast area of crossfertilization of ideas between biologists, chemists, and theoretical physicists. Results of single-molecule experiments have posed challenges to theoretical physicists who have combined ideas from statistical mechanics, quantum mechanics, differential geometry, and topology to get a proper understanding of the field.

Bustamante et al. directly measured the elasticity of a single DNA molecule by attaching one end of the molecule to a glass slide and the other end to a micron size magnetic bead [17]. A stretching force was applied to the DNA molecule by applying a magnetic field gradient and the corresponding extension was measured by observing the position of the bead under an optical microscope. The mechanical response of such a system was, thus, probed in the form of a force-extension curve. The experimental curves were compared first against the simplest theory available for a polymer—the freely jointed chain (FJC) in which the polymer is viewed as a chain of rigid rods connected by revolving pivots. While the experimental curves agreed well with the FJC model at low forces, the comparison showed considerable discrepancies between theory and experimental curves in the intermediate and large force regime. This pointed toward a deficiency in the theory which was subsequently remedied by Marko and Siggia who used the worm-like chain (WLC) model [19]. In the WLC model, one takes into consideration the bending energy $\left(\mathcal{E} = \frac{1}{2}A\int_0^L \mathrm{d}s\kappa^2\right)$ with $A = L_\mathrm{p}k_\mathrm{B}T$ the bending modulus) proportional to the square of the curvature κ of the space curve representing the polymer of contour length L kept at a temperature T. L_p, the persistence length is a measure of the rigidity of the polymer and it is the length scale over which the polymer can be considered to be essentially straight. The WLC model provided excellent quantitative agreement with the experimental force–extension curves [17]. This pointed to the fact that a DNA molecule needs to be viewed as a semiflexible (partly flexible and partly stiff) polymer rather than a completely flexible one. There is a vast literature on semiflexible polymer elasticity [20].

4.2 DNA twist statistics

In the experiments of Strick and collaborators [21], the ends of a single molecule of double-stranded DNA are attached to a glass plate and a magnetic bead. Magnetic fields are used to control the orientation of the bead and magnetic field gradients to apply forces on the bead. By such techniques, the molecule is stretched and twisted and the extension of the molecule is monitored by the location of the bead. A typical experimental run measures the extension of the molecule as a result of the applied twist and force. These experiments are important toward an understanding of the role of twist elasticity in biological processes like DNA replication. In laboratory and biological conditions, the thermal fluctuations of the DNA molecule are important and it is necessary to take these into account to understand the experiments of Strick et al. To determine the response of a DNA molecule to twist and stretch, one has to calculate its partition function: sum over all possible configurations of the molecule with Boltzmann weight $\exp[-E/kT]$. As Strick et al remark that is a tall order, not likely to be filled anytime soon. Computer simulations of the system are possible and have been done. These simulations, which incorporate realistic features like self-avoidance, agree well with laboratory experiments and can be viewed in two ways. From the point of view of a laboratory experimenter, they are like theoretical models. From a theorist's standpoint simulations can be viewed as controlled experiments. The main theoretical difficulty is the incorporation of self-avoidance, which is present in a real DNA molecule: the conformation of the molecule must never intersect itself. Such a constraint is virtually impossible to handle theoretically, and one is forced to resort to simpler models. Although the agreement with the experimental curves is good there are some issues related to self-avoidance of the polymer [22] which are still poorly understood and one needs to introduce an adjustable cut-off parameter to fit the experimental curves. The significance of this cut-off parameter is not entirely clear and there are open issues yet to be understood.

In the past, experiments on biopolymers were confined to studying their bulk properties, which involved probing large numbers of molecules. The results of these experiments could be analyzed by using the traditional tools of thermodynamics. However, when one micromanipulates single polymer molecules the usual rules of thermodynamics applicable to bulk systems no longer hold. Single molecule experiments thus provide physicists with a concrete testing ground for understanding some of the fundamental ideas of statistical mechanics. In particular, fluctuations about the mean value of a variable play an important role due to the finite extent of the molecule. For instance, it turns out, that an experiment in which the distance between the ends of a polymer molecule is fixed (an isometric setup) and the tension fluctuates yields a different "equation of state" from one in which the tension between the ends is held fixed (an isotensional setup) and the end-to-end distance fluctuates. This asymmetry can be traced to large fluctuations about the mean value of the force or the extension, depending on the experimental setup [23, 24]. These fluctuations vanish only in the thermodynamic limit of very long polymers. A similar effect is seen in experiments involving twisting DNA molecules. If the DNA is short enough, experiments with a fixed torque and a fluctuating twist give a different Torque–Twist Relation from those with a fixed twist and a fluctuating torque [25].

4.3 Verification of Jarzynski's equality

We will now come to an interesting connection between equilibrium and nonequilibrium statistical mechanics which has emerged in recent years and its relevance to single-molecule experiments. It has been proved [26, 27] that a remarkable equality exists, relating work done in a series of finite time, nonequilibrium measurements and the equilibrium free energy difference between two given configurations of a system. What is most remarkable is, unlike linear response and the fluctuation–dissipation theorem which relate equilibrium statistical mechanics to nonequilibrium processes close to equilibrium, this relation is valid arbitrarily far from equilibrium. Let us consider a finite classical system that depends on an external parameter λ. Let the system come to equilibrium with a reservoir at a temperature T. If we now switch the external parameter from an initial value $\lambda = 0$ to a final value $\lambda = 1$ infinitely slowly then the work W_∞ done on the system is given by: $W_\infty = \Delta F = F_1 - F_0$ where F_λ is the Free energy of the system at a temperature T at a fixed value of λ. Let us now consider switching the parameter λ at a finite rate. In such a situation the system is no longer in quasistatic equilibrium with the reservoir at every stage. The work done in such a case *depends* on the microscopic initial conditions of the system and the reservoir. One now needs to consider an *ensemble* of such switching measurements and the total work done is no longer equal to the free energy difference but always exceeds it.

It turns out, however, that a remarkable equality still holds connecting the work done in such a process and the difference between the initial and final values of the free energy. The equality, known as Jarzynski's equality is given by: $\overline{\exp(-\beta W)} = \exp(-\beta \Delta F)$. The overbar on the left pertains to an ensemble average over all possible finite time measurement realizations.

Liphardt and collaborators [28] have tested the validity of this remarkable equality via single-molecule experimental measurements. They tested the equality by comparing work done in reversible and irreversible unfolding of a single RNA molecule. Small beads were attached at the ends of a single RNA molecule. The bead at one end was held in an optical trap. By measuring the displacement δ of the bead in the trap and the stiffness constant k

of the trap, the force $F = k\delta$ on the molecule was measured. The bead at the other end was held by a micropipette and attached to a piezoelectric device which enabled the position of the bead to be controlled by varying the voltage. The position z of the second bead relative to a given reference point was used to measure the extent of unfolding of the molecule. The work W done was measured by integrating the product of the force and the displacement and plotted as a function of the extension z. The experiment was repeated at varying rates of pull. There were essentially two classes of measurements: quasistatic, near equilibrium measurements where the work done was reversible and given by the free energy difference between the two end values of the control parameter and the other class consisted of measurements carried out at faster rates of pull (truly nonequilibrium situation) where the molecule does not have time to equilibriate during pulling. The experimenters took an average over all possible realizations of the nonequilibrium measurements and evaluated the quantity $\overline{\exp(-\beta W)}$ and compared it against its equilibrium counterpart $\exp(-\beta \Delta F)$ and found good agreement within experimental error corroborating Jarzynski's equality.

5 Active Brownian motion

In recent years, Active Matter has emerged as a significant area of research [30]. Active particles are self-propelled particles which generate dissipative directed motion by consuming energy from the environment. There are many examples of Active Matter in Soft Matter and biological systems like bacterial run and tumble motion, swimming microbes, schools of fish, swarms of birds, driven granular matter, and so on.

There are two approaches toward understanding the physics of Active Matter. One approach is a coarse-grained hydrodynamic approach where one looks at the collective dynamics of Active Matter [29, 30]. The other approach involves studying the dynamics of a single active Brownian particle [31–33]. There has been a considerable amount of theoretical, simulational and experimental work in this area both at the large scale hydrodynamic level [34, 35]and at the level of single-particle dynamics [30].

An active overdamped particle in two dimensions moving at a constant speed v_0 is characterized by its position coordinates (x, y) and an "active" internal degree of freedom, given by the orientational angle $\phi(t)$ of its velocity, which undergoes rotational diffusion. The time evolution is given by the following Langevin equations [29, 36, 37]:

$$\dot{x} = v_0 \cos\phi(t), \tag{7}$$

$$\dot{y} = v_0 \sin\phi(t), \tag{8}$$

$$\dot{\phi} = \sqrt{2D_{\mathrm{R}}}\eta_\phi(t), \tag{9}$$

where $\eta_\phi(t)$ is a Gaussian white noise with zero mean and correlator $\langle \eta_\phi(t)\eta_\phi(t')\rangle = \delta(t-t')$. The rotational diffusion sets a persistence time scale D_{R}^{-1} for the dynamics of the spatial coordinates of an active Brownian particle (ABP). It has been seen [32] that, while for $t >> D_{\mathrm{R}}^{-1}$ the ABP dynamics reduces to an ordinary two dimensional Brownian motion, signatures of activity show up for $t << D_{\mathrm{R}}^{-1}$ where the dynamics is seen to be anisotropic and there are strong correlations present between the x and y coordinates (see Fig. 1–Fig. 3 in Ref. [32]).

One can show that there is an exact mapping between ABP dynamics and equilibrium properties of a WLC polymer [38]. The persistence length L_P of a WLC polymer is the counterpart of the persistence time D_{R}^{-1} for an ABP. In the realm of equilibrium statistical mechanics of a WLC semiflexible polymer, one notices an interesting transition from a double humped profile to a single peaked Gaussian profile as one changes the ratio of the contour length L and the persistence length L_{P} [6, 39]. An analogous transition takes place for an ABP as one changes the ratio r of the observation time t and the persistence time D_{R}^{-1}. The position probability distribution undergoes a qualitative change as one changes r. In particular, the late time dynamics of a single active Brownian particle in two dimensions with speed v_0 and rotational diffusion constant D_{R} has been studied and it has been shown that at late times $t >> D_{\mathrm{R}}^{-1}$ while the position probability distribution $P(x, y, t)$ in the $x-y$ plane approaches a Gaussian form near its peak describing the typical diffusive fluctuations, it has non-Gaussian tails describing atypical rare fluctuations when $\sqrt{x^2+y^2} \sim v_0 t$. Another way of detecting activity at late times is to subject the active particle to an external harmonic potential. In this case, one can show that the stationary distribution $P_{stat}(x, y)$ depends explicitly on the activity parameter $D_{\mathrm{R}}^{-}1$ and undergoes a crossover, as D_{R} increases, from a ring shape in the strongly active limit ($D_{\mathrm{R}} \to 0$) to a Gaussian shape in the strongly passive limit ($D_{\mathrm{R}} \to \infty$) [40].

Apart from the position probability distributions discussed above, orientational probability distributions of an ABP have also been studied [41, 42]. In three dimensions, the Fokker–Planck equation for the orientational

probability distribution of an ABP is [42]:

$$\frac{\partial P(\theta,\,\phi,\,t)}{\partial t} = D_{\mathrm{R}}\left[\frac{1}{\sin\theta}\frac{\partial}{\partial\theta}\left(\sin\theta\frac{\partial P}{\partial\theta}\right) + \frac{1}{\sin^2\theta}\frac{\partial^2 P}{\partial\phi^2}\right]. \tag{10}$$

The Fokker–Planck equation has the following exact solution as kernel in series form [41]:

$$\begin{aligned} &K(\theta_0,\,\phi_0,\,0,\,\theta,\,\phi,\,t) \\ &\quad = \sum_{l=0}^{\infty}\sum_{m=-l}^{l} e^{-D_{\mathrm{R}}l(l+1)t}Y_l^{m^*}(\theta_0,\,\phi_0)Y_l^m(\theta,\,\phi). \end{aligned} \tag{11}$$

An azimuthally symmetric initial distribution $P(\theta,\,0)$ leads to a simpler form for the series solution [41]

$$P_{\mathrm{exact}}(\theta,\,t) = \frac{\sin\theta}{2}\sum_{l=0}^{\infty}(2l+1)e^{-\frac{l(l+1)t}{2}}P_l(\cos\theta), \tag{12}$$

where we have included the measure $\sin\theta$ and set $D_{\mathrm{R}} = \frac{1}{2}$. Although the solution in the above equation is exact, poor convergence at short times is expected to come in the way of an effective implementation in the short time domain.

The orientational probability distribution for an active Brownian particle discussed here involves a kernel for diffusion on a sphere where the end points lie on the sphere. This can be viewed as a Wiener path integral [5] problem where one sums over all possible paths between the two end points. One can arrive at a short time approximate form for the orientational probability distribution of an ABP via a semiclassical approximation involving the Van Vleck fluctuation determinant. The semiclassical approximation (a saddle point approximation) discussed here involves restriction to quadratic fluctuations around the classical path (a geodesic on the sphere) captured by the Van Vleck determinant. This approximate expression can be implemented effectively at short and intermediate times [42, 43].:

$$P^S_{\mathrm{approx}}(\theta,\,t) = \frac{N(t)}{t}\sqrt{\theta\sin\theta}e^{-\frac{\theta^2}{2t}}. \tag{13}$$

Notice that in contrast to $P_{\mathrm{exact}}(\theta,\,t)$ where time t appears in the numerator of the argument of the exponential, the analytical form of the approximate propagator $P^S_{\mathrm{approx}}(\theta,\,t)$ has much better convergence properties at short times because of the appearance of time in the denominator of the argument of the exponential. One can see by plotting this function via Mathematica and comparing it with the plot of the exact orientational probability distribution that this approximate short time formula in fact works remarkably well even at intermediate times (see Figs. 3 and 4) [42].

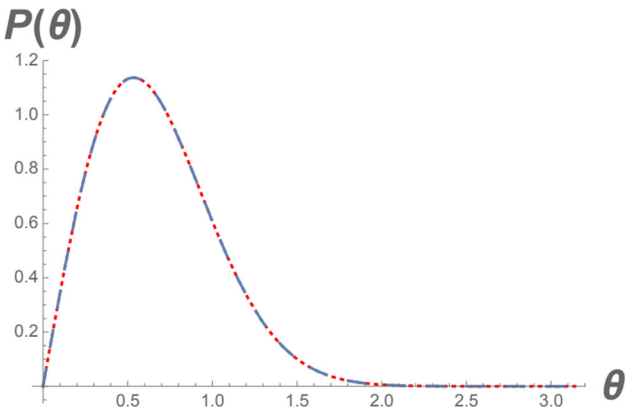

Fig. 3 Comparison of the short time approximate orientational probability distribution (red dotted line) and the exact orientational probability distribution (blue dashed line) of an ABP at time $t = 0.3$

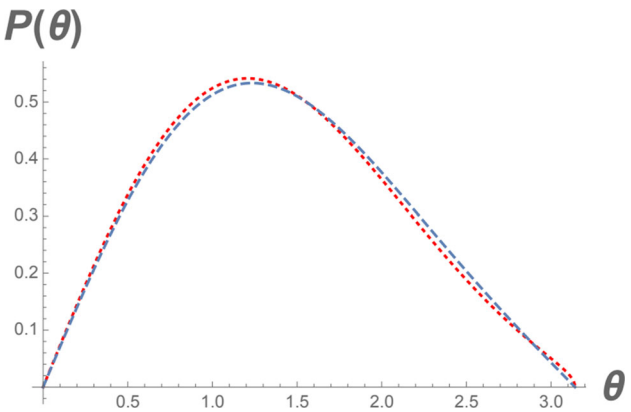

Fig. 4 Comparison of the short time approximate orientational probability distribution (red dotted line) and the exact orientational probability distribution (blue dashed line) of an ABP at time $t = 10$

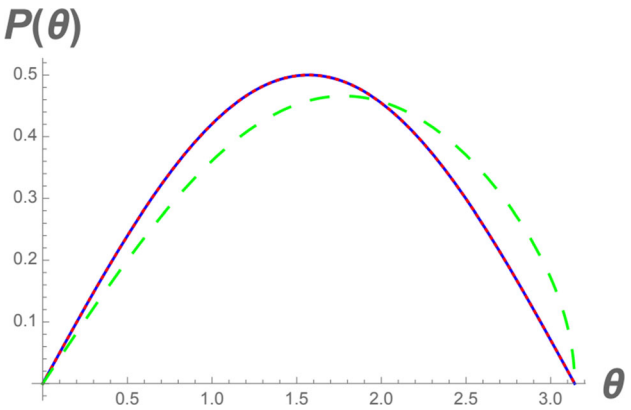

Fig. 5 Comparison of the short time approximate orientational probability distribution (green dashed line), the exact orientational probability distribution (blue line) and the long time approximate orientational probability distribution (red dotted line) of an ABP at time $t = 10$. Notice that the curves for the long time approximate orientational probability distribution (red) and the exact orientational Probability distribution (blue) lie on top of one another

One can also arrive at a long time approximate form for the orientational probability distribution:

$$P^{L}_{\text{approx}}(\theta, t) = \frac{1}{2}\left[\sin\theta\left(1 - \frac{5}{2}e^{-3t}\right) + \left(\frac{3\sin 2\theta}{2}\right)\left(e^{-t} + \frac{5}{2}\cos\theta e^{-3t}\right)\right]. \tag{14}$$

This is an approximate analytical form which works very well in the long time limit (see Fig. 5) [42].

5.1 Collective dynamics of active particles

We now briefly discuss some work in which the collective dynamics of active particles has been analyzed [44–46]. For instance, motivated by simulations and experiments on aggregation of gliding bacteria, a model of the collective dynamics of self-propelled hard rods on a substrate in two dimensions has been analyzed theoretically [44]. The rods have finite size, interact via excluded volume, and their dynamics is overdamped by the interaction with the substrate. Starting from a microscopic model with nonthermal noise sources, a continuum description of the system has been derived. The hydrodynamic equations have then been used to characterize the possible steady states of the systems and their stability as a function of the particle packing fraction and the speed of self-propulsion.

In [45], the authors have started from a microscopic model and arrived at a continuum field theoretic description of the dynamics of a system of active ingredients or particles. The equations of motion for the respective collective densities of mass and momentum follow exactly from that of a single element in the flock. Flocking or the collective, coherent motion of large numbers of self-propelled particles have been studied. These exhibit distinct 'phases' which are characterized by distinct symmetry properties [46]. One of the intriguing features of these Active Matter

systems is the presence of giant number fluctuations which grow with the number of organisms faster than $\sqrt{N}$ that are typically seen in most systems.

6 Concluding remarks

We summarize the topics highlighted in this review. We started with a discussion of a set of pioneering experiments by Agnes Pockels in the domain of Soft Matter, as an introduction to the general area of Soft Matter. In subsequent sections, we have given a perspective on Soft Matter physics by focusing on a few topics which have their origin in Brownian motion, a foundational pillar of statistical mechanics and Soft Matter physics.

We first discussed Brownian motion on a sphere and then discussed a few topics in subsequent sections where we applied the idea of Brownian motion on a sphere to two distinct Soft Matter systems: semiflexible biopolymers and active Brownian motion. As mentioned in the Introduction, the worm-like chain model is a model of an inextensible semiflexible polymer which maps to the problem of Brownian motion on a sphere, where the tangent vectors to the curve representing the polymer form a unit sphere. Thus the problem reduces to studying Brownian motion on the unit sphere. The orientational degree of freedom of an active Brownian particle undergoes rotational diffusion and, thus, the orientational distribution function of an active Brownian particle is equivalent to the angular distribution function for diffusion on a sphere. Thus Brownian motion, in particular Brownian motion on a sphere is the common thread connecting the various topics discussed in Sects. 3, 4 and 5.

Needless to say, this article is not meant to be an exhaustive survey of all topics in Soft Matter. It introduces the reader to a few topics in Soft Matter which are intertwined by the common thread of Brownian motion.

We expect the review article to generate interest in researchers working in the area of Soft Matter to pursue some of the topics of current interest.

References

1. T. McLeish, *Soft Matter: A Very Short Introduction* (Oxford University Press, Oxford, 2020)
2. P. Nelson, B. Physics, *Energy, Information, Life* (W. H. Freeman, New York, 2007)
3. N. Byers, G. Williams, *Out of the Shadows: Contributions of Twentieth-Century Women to Physics* (Cambridge University Press, Cambridge, 2010), pp.36–42
4. A. Einstein, *Investigations on the Theory of the Brownian Movement* (Courier Corporation, North Chelmsford, 1956)
5. L.S. Schulman, *Techniques and Applications of Path Integration* (Dover Books on Physics, Mineola, 2005)
6. J. Samuel, S. Sinha, Phys. Rev. E **66**, 050801 (2002)
7. S. Sinha, J. Samuel, Phys. Rev. B **50**, 13871(R) (1994)
8. M.M.G. Krishna, J. Samuel, S. Sinha, J. Phys. A Math. Gen. **33**, 5965 (2000)
9. M.M.G. Krishna, R. Das, N. Periasamy, R. Nityananda, J. Chem. Phys. **112**, 8502–8514 (2000)
10. F. Wilczek, A. Shapere, *Geometric Phases in Physics* (World Scientific, Singapore, 1989)
11. P.W. Kuchel, A.J. Lennon, C. Durrant, J. Magn. Reson. B **112**, 1–17 (1996)
12. M.G. Brereton, C. Butler, J. Phys. A (Lond.) **20**, 3955 (1987)
13. D.C. Khandekar, F.W. Wiegel, Physica A **193**, 421 (1993)
14. N. Wiener, J. Math. Phys. **2**, 132 (1923)
15. D. Maxim, F. Kamenetskii, *Unraveling DNA: The Most Important Molecule of Life* (Basic Books, New York, 1997)
16. B. Alberts, A. Johnson, J. Lewis, M. Raff, K. Roberts, P. Walter, *Molecular Biology of the Cell* (Garland Science, New York, 2002)
17. C. Bustamante, S.B. Smith, J. Liphardt, D. Smith, Current Opinion in Structural Biology **10**, 279 (2000)
18. P. Hinterdorfer, A. Oijen, N. Dekker, D. Muller, T. Schmidt, C. Seidel, S. Xie, C. Zhu, X. Zhuang, *Handbook of Single-Molecule Biophysics* (Springer, New York, 2009)
19. J.F. Marko, E.D. Siggia, Macromolecules **28**, 8759 (1995)
20. J. David Moroz, P. Nelson, PNAS **94**, 14418 (1997)
21. T.R. Strick, J.F. Allemand, D. Bensimon, A. Bensimon, V. Croquette, Science **271**, 1835–7 (1996)
22. J. Samuel, S. Sinha, A. Ghosh, J. Phys. Condens. Matter **18**, S253 (2006)
23. H.J. Kreuzer, S.H. Payne, L. Livadaru, Biophys. J. **80**, 2505 (2001)
24. S. Sinha, J. Samuel, Phys. Rev. E **71**, 021104 (2005)
25. S. Sinha, Phys. Rev. E **296**, 1832 (2002)
26. G.N. Bochkov, Y.E. Kuzovlev, Sov. J. Exp. Theor. Phys. **45**, 125–130 (2021)
27. C. Jarzynski, Phys. Rev. Lett. **78**, 2690–2693 (1997)
28. J. Liphardt, S. Dumont, S.B. Smith, I. Tinoco Jr., C. Bustamante, Science **296**, 1832 (2002)
29. S. Ramaswamy, J. Stat. Mech. **2017**, 054002 (2017)
30. M.C. Marchetti, J.F. Joanny, S. Ramaswamy, T.B. Liverpool, J. Prost, M. Rao, R. Aditi Simha, Rev. Mod. Phys. **85**, 1143 (2013)

31. D. Chaudhuri, A. Dhar, J. Stat. Mech. **2021**, 013207 (2021)
32. U. Basu, S.N. Majumdar, A. Rosso, G. Schehr, Phys. Rev. E **98**, 062121 (2018)
33. I. Santra, U. Basu, S. Sabhapandit, Phys. Rev. E **104**, L012601 (2021)
34. F. Jülicher, S.W. Grill, G. Salbreux, A.J. Lennon, C. Durrant, Rep. Progr. Phys. **81**, 076601 (2018)
35. O. Hallatschek, S.S. Datta, K. Drescher, J. Dunkel, J. Elgeti, B. Waclaw, N.S. Wingreen, Nat. Rev. Phys. **5**, 407 (2023)
36. C. Bechinger, R. Di Leonardo, H. Löwen, C. Reichhardt, G. Volpe, G. Volpe, Rev. Mod. Phys. **88**, 045006 (2016)
37. E. Fodor, M.C. Marchetti, Phys. A (Amsterdam) **504**, 106 (2018)
38. A. Shee, A. Dhar, D. Chaudhuri, Soft Matter **16**, 4776–4787 (2020)
39. A. Dhar, D. Chaudhuri, Phys. Rev. Lett. **89**, 065502 (2002)
40. U. Basu, S.N. Majumdar, A. Rosso, G. Schehr, Phys. Rev. E **98**, 062121 (2018)
41. X. Zheng, B. ten Hagen, A. Kaiser, W. Meiling, H. Cui, Z. Silber-Li, H. Löwen, Phys. Rev. E **88**, 032304 (2013)
42. S. Sinha, J. Stat. Mech. Theory Exp. **2020**, 083201 (2020)
43. A. Ghosh, J. Samuel, S. Sinha, Europhys. Lett. **98**, 30003 (2012)
44. A. Baskaran, M. Cristina Marchetti, Phys Rev. E **77**, 011920 (2008)
45. S. Kumar Yadav, S.P. Das, Phys. Rev. E **97**, 032607 (2018)
46. M.J. Bowick, N. Fakhri, M.C. Marchetti, S. Ramaswamy, Phys. Rev. X **12**, 010501 (2022)